Journal of Clinical Neurophysiology
19(4):361–370, Lippincott Williams & Wilkins, Inc., Philadelphia

A Coil Design for Transcranial Magnetic Stimulation of Deep Brain Regions

Yiftach Roth,* Abraham Zangen,† and Mark Hallett‡

**New Advanced Technology Center, Sheba Medical Center Tel-Hashomer, Israel; †National Institute on Drug Abuse, National Institutes of Health, Baltimore, Maryland, U.S.A.; ‡National Institute of Neurological Disorders and Stroke, National Institutes of Health, Bethesda, Maryland, U.S.A.*

Summary: Noninvasive magnetic stimulation of the human central nervous system has been used in research and the clinic for several years. However, the coils used previously stimulated mainly the cortical brain regions but could not stimulate deeper brain regions directly. The purpose of the current study was to develop a coil to stimulate deep brain regions. Stimulation of the nucleus accumbens and the nerve fibers connecting the prefrontal cortex with the nucleus accumbens was one major target of the authors' coil design. Numeric simulations of the electrical field induced by several types of coils were performed and accordingly an optimized coil for deep brain stimulation was designed. The electrical field induced by the new coil design was measured in a phantom brain and compared with the double-cone coil. The numeric simulations show that the electrical fields induced by various types of coils are always greater in cortical regions (closer to the coil placement); however, the decrease in electrical field within the brain (as a function of the distance from the coil) is markedly slower for the new coil design. The phantom brain measurements basically confirmed the numeric simulations. The suggested coil is likely to have the ability of deep brain stimulation without the need to increase the intensity to levels that stimulate cortical regions to a much higher extent and possibly cause undesirable side effects.
Key Words: Deep brain stimulation—Magnetic coil—Tranascranial magnetic stimulation—Electrical field—Nucleus accumbens—Reward.

Accumulating evidence suggests that the nucleus accumbens plays a major role in mediating reward and motivation (Breiter and Rosen, 1999; Ikemoto and Panksepp, 1999; Kalivas and Nakamura, 1999; Schultz et al., 1997; Self and Nestler, 1995). Functional MRI and positron emission tomographic studies showed that the nucleus accumbens is activated in cocaine addicts in response to cocaine administration (Breiter et al., 1997; Lyons et al., 1996). Other brain regions are also associated with reward circuits, such as the ventral tegmental area, amygdala, and medial prefrontal, cingulate, and orbitofrontal cortices (Breiter and Rosen, 1999; Kalivas and Nakamura, 1999). Moreover, neuronal fibers connecting the medial prefrontal, cingulate, or orbitofrontal cortex with the nucleus accumbens may have an important role in reward and motivation (Jentsch and Taylor, 1999; Volkow and Fowler, 2000). The nucleus accumbens is also connected to the amygdala and the ventral tegmental area. Therefore, activation of these brain regions may affect neuronal circuits mediating reward and

Abraham Zangen and Yiftach Roth contributed equally to the study.

A provisional patent application was filed on October 20, 2000. A PCT international application (no. PCT/US01/05737)was filed on October 19, 2001. The National Institutes of Health (no. 60/242,297; Department of Health and Human Services) reference no. is E-223-00/0.

Address correspondence and reprint requests to Dr. Abraham Zangen, National Institute on Drug Abuse, National Institutes of Health, 5500 Nathan Shock Drive, Baltimore, MD 21224 U.S.A.; e-mail: azangen@intra.nida.nih.gov

motivation. In rats and monkeys and even in humans, electrical stimulation of the median forebrain bundle is rewarding, and when a stimulating electrode is inserted into various parts of that bundle (including the ventral tegmental area, the median prefrontal cortex and the nucleus accumbens septi), compulsive self-stimulation can be obtained (Jacques, 1999; Milner, 1991).

Transcranial magnetic stimulation is a noninvasive technique used to apply magnetic pulses to the brain. The pulses are administered by passing high currents through an electromagnetic coil placed on the scalp that can induce electrical currents in the underlying cortical tissue, thereby producing a localized axonal depolarization. During the last 5 years, this technique has been applied to studying and treating various neurobehavioral disorders, primarily mood disorders (Kircaldie et al., 1997; Wassermann and Lisanby, 2001). The coils used for TMS (mostly the figure-of-eight coil) induce stimulation in cortical regions mainly just superficially under the windings of the coil. The intensity of the electrical field drops dramatically deeper in the brain as a function of the distance from the figure-of-eight or the circular coils (Cohen et al., 1990; Eaton, 1992; Maccabee et al., 1990; Tofts, 1990; Tofts and Branston, 1991). The use of an array of circular or figure-of-eight coils placed parallel to the skull can in some cases improve the focality of the field at the cortex, but does not improve the stimulation in depth (Ruhonen and Ilmoniemi, 1998). The so-called *slinky coil* is composed of several windings in intermediate orientation between the figure-of-eight coil parallel to the surface and the circular coil perpendicular to the surface. It can achieve larger field magnitude and better focality at the cortex near the coil center, but has no advantage for deep brain stimulation (Ren et al., 1995; Zimmermann and Simpson, 1996).

Therefore, to stimulate deep brain regions, a very high intensity would be needed. Such intensity cannot be reached by standard magnetic stimulators using the regular figure-of-eight or circular coils. Moreover, the intensity needed to stimulate deeper brain regions effectively would stimulate cortical regions and facial nerves over the level that may lead to facial pain, facial and cervical muscle contractions, and other undesirable side effects.

The double-cone coil has a somewhat similar shape as the figure-of-eight coil except that the two rings create an angle (95 deg) between them and their diameter is usually larger. This coil, which is able to create a greater electrical field intensity, is considered to be the best tool for stimulation of deeper brain regions compared with other coils, and was reported to have the ability to stimulate the leg motor area, which is 3 to 4 cm in depth (Stokic et al., 1997; Terao et al., 1994, 2000).

Electrical field intensity in the tissue and the rate of decrease of electrical field as function of distance from the coil, depend strongly on the orientation of coil elements relative to tissue surface. Studies with volume conductors having flat (Branston and Tofts, 1990; Roth et al., 1990; Tofts, 1990; Tofts and Branston, 1991) and spherical (Branston and Tofts, 1991; Cohen and Cuffin, 1991; Eaton, 1992) geometries have demonstrated that coil elements perpendicular to the surface induce accumulation of surface charge, which leads to complete cancellation of the perpendicular component of the induced field at all points within the tissue. In addition, the electrical field in any other direction is considerably reduced.

Therefore, when designing a coil for deep brain stimulation, an effort should be made to minimize the overall length of coil elements that are not tangential to brain tissue surface. Physiologic studies of peripheral nerves revealed that optimal activation occurs when the field is oriented in the same direction as the nerve fiber (Basser and Roth, 1991; Roth and Basser, 1990). Hence, to stimulate deep brain regions, it is necessary to use coils in such an orientation that they will produce a considerable field in a direction tangential to the surface, which should also be the preferable direction to activate the neurons under consideration. Another requirement is that the field in the deep region will be as large as possible compared with the field at the cortex.

In this study we introduce a new coil (termed the *Hesed coil*) that is designed to stimulate effectively deeper brain regions without increasing the electrical field intensity in the superficial cortical regions. We present numeric simulations and phantom measurements of the total electrical field produced by the Hesed coil inside a homogeneous spherical volume conductor and compare these with results from a circular coil in different orientations and from the double-cone coil. The drop of the electrical field in the brain as a function of the distance from the new coil is much slower compared with previous coils. It is hoped that such a coil can stimulate deeper regions such as the nucleus accumbens and the fibers connecting the medial prefrontal or cingulate cortex with the nucleus accumbens. Activation of these fibers may induce reward, and chronic treatment may have antidepressant properties or serve as a new strategy against drug addiction.

METHODS

Electromagnetic Framework

We consider the steady-state effect of a transcranial magnetic stimulation coil on the brain. We assume that the brain is a homogeneous volume conductor with permeability of free space μ_0 and permissiveness much larger than that of free space ε_o. We also treat the skull as a complete insulator with permissiveness of ε_o.

For magnetic stimulation of the brain or peripheral nerves, a brief high current should be passed through a coil of wire, generating a time-varying magnetic field. The vector potential A(r) in position r is related to the current in a wire I by the equation

$$A(r) = \frac{\mu_0 I}{4\pi} \int \frac{dl'}{|r - r'|} \quad (1)$$

where $\mu_0 = 4\pi \times 10^{-7}$ Tm/A is the permeability of free space, the integral of dl' is over the wire path, and r' is a vector indicating the position of the wire element. The magnetic and electrical fields are related to the vector potential through the equations

$$B_A = \nabla \times A \quad (2)$$

$$E_A = -\frac{\partial A}{\partial t} \quad (3)$$

Because brain tissue has conducting properties, whereas the air and skull are almost complete insulators, the vector potential will induce an accumulation of electrical charge at the brain surface, unless the induced electrical field is completely tangential to the brain surface at every point. This charge is another source for the electrical field, which can be expressed as

$$E_\phi = -\nabla\Phi \quad (4)$$

where Φ is the scalar potential produced by the surface electrostatic charge. The total field in the brain tissue E is the vectorial sum of these two fields:

$$E = E_A + E_\Phi \quad (5)$$

The influence of the electrostatic field E_Φ is in general opposite to the induced field E_A and consequently reduces the total field E. The amount of surface charge produced and hence the magnitude of E_Φ depends strongly on coil configuration and orientation.

Numeric Simulations

The simulations were conducted using a Mathematica program (Mathematica version 4.0, 1999; Wolfram Research Inc., Champaign, IL, U.S.A.). The head was modeled as a spherical homogeneous volume conductor with a radius of 7 cm. The induced and electrostatic field at a specific point inside the spherical volume were computed for several coil configurations, using the method presented by Eaton (1992), and the total electrical fields in the x (Ex), y (Ey), and z (Ez) directions were calculated (Fig. 1).

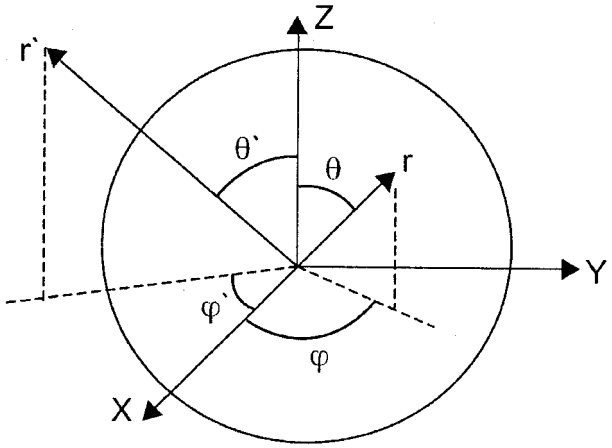

FIG. 1. The relation between the spherical coordinate system and the Cartesian coordinate system for which the field components in every point were calculated. R is the radius vector to the point inside the sphere where the field is computed, and r' is the vector to the differential coil element on which the integration is performed.

The vector potential A and scalar potential Φ can be expanded in terms of spherical harmonic functions up to N order. After enforcing the boundary conditions at the sphere boundary, the final expressions for the total electrical field in the three Cartesian directions are

$$E_j = E_{Aj} + E_{\Phi j} \quad (6)$$

$$j = x, y, z \quad (7)$$

where the induced field in each direction is given by

$$E_{Aj} = -\mu_0 \frac{\partial I}{\partial t} \sum_{l=0}^{N} \sum_{m=-1}^{1} r^l Y_{lm}(\theta, \varphi) C_{lm}^{\ j} \quad j = x, y, z \quad (8)$$

where $Y_{lm}(\theta,\phi)$ are spherical harmonic functions; r, θ, and ϕ are spherical coordinates of the point inside the conductive sphere where the electrical field is calculated (see Fig. 1); and $C_{lm}^{\ j}$ are j− component of the integration over the coil path:

$$C_{lm}^{\ j} = \int_{coil} \frac{Y^*_{lm}(\theta', \varphi')dlj}{(2l+1)r'^{l+1}} \quad j = x, y, z \tag{9}$$

where * means complex conjugate, r', θ', and ϕ' are spherical coordinates of the coil element (see Fig. 1), and dlj is the j component of the differential element of the coil. The electrostatic fields in x, y and z directions are given by

$$E_{\Phi x} = -\sin(\theta)\cos(\varphi)\sum_{l=1}^{N+1}\sum_{m=-1}^{1} V_{lm} l r^{l-1} Y_{lm}(\theta,\varphi) +$$

$$\cos(\theta)\cos(\varphi)\sum_{l=1}^{N+1}\sum_{m=-1}^{1} V_{lm} r^{l-1} \_[\exp(i\varphi)\sqrt{((1-m+1)(1+m))} Y_{l,m-1}(\theta,\varphi) - \exp(-i\varphi)\sqrt{((1+m+1)(1-m))} Y_{l,m+1}(\theta,\varphi)]$$

$$+ \frac{\sin(\varphi)}{\sin(\theta)}\sum_{l=1}^{N+1}\sum_{m=-1}^{l} V_{lm} r^{l-1} i m Y_{lm}(\theta,\Phi) \tag{10}$$

$$E_{\Phi y} = -\sin(\theta)\sin(\varphi)\sum_{l=1}^{N+1}$$

$$\sum_{m=-1}^{1} V_{lm} 1 r^{l-1} Y_{lm}(\theta,\varphi)$$

$$+ \cos(\theta)\sin(\varphi)\sum_{l=1}^{N+1}\sum_{m=-1}^{1} V_{lm} r^{l-1} \_[\exp(i\varphi)\sqrt{((1-m+1)(1+m))} Y_{l,m-1}(\theta,\varphi) - \exp(-i\varphi)\sqrt{((1+m+1)(1-m))} Y_{l,m+1}(\theta,\varphi)]$$

$$- \frac{\cos(\varphi)}{\sin(\theta)}\sum_{l=1}^{N+1}\sum_{m=-1}^{1} V_{lm} r^{l-1} i m Y_{lm}(\theta,\varphi) \tag{11}$$

$$E_{\Phi z} = -\cos(\theta)\sum_{l=1}^{N+1}\sum_{m=-1}^{1} V_{lm} l r^{l-1} Y_{lm}(\theta,\varphi)$$

$$- \sin(\theta)\sum_{l=1}^{N+1}\sum_{m=-1}^{1} V_{lm} r^{l-1} \_[\exp(i\varphi)\sqrt{((1-m+1)(1+m))} Y_{l,m-1}(\theta,\varphi) - \exp(-i\varphi)\sqrt{((1+m+1)(1-m))} Y_{l,m+1}(\theta,\varphi)] \tag{12}$$

Where $i = \sqrt{-1}$, and V_{lm} is a complex function of the integrals over coil path $C_{lm}^{\ j}$:

$$V_{lm} = -\frac{\mu_0}{1}\frac{\partial I}{\partial t}(\sqrt{[(1+m-1)(1+m)/((2l+1)(2l-1))]} 0.5(C_{l-1,m-1}^{\ y} i - C_{l-1,m-1}^{\ x}) + \sqrt{[(1-m-1)(1-m)/((2l+1)(2l-1))]} 0.5(C_{l-1,m+1}^{\ y} i + C_{l-1,m+1}^{\ x}) + \sqrt{[(1-m)(1+m)/((2l+1)(2l-1))]} C_{l-1,m}^{\ z}) \tag{13}$$

The simulations were performed using 10th order approximation. The summations in Eqs. 8 to 13 were computed up to N = 10. The convergence rate depends on the distance from coil elements and on coil configuration, and in general, is faster for more remote points. For the new coil design, the convergence rate was faster than for the circular coil. For points close to the coils (up to 1.5 cm), the induced field was corrected by the exact formula (Eq. 3). For more remote points the error was less than 1%. In all the calculations, the rate of current change was taken as 10,000 amps/100 μsec (which is approximately the maximal power output of standard stimulators). The field is given in volts per meter.

Measurements of the Electrical Field Induced in a Phantom Brain

The electrical field induced by the new coil and the double-cone coil (Magstim; Whitland, UK) was measured in a saline solution placed in a hollow glass model of the human head (15 × 17 × 20 cm; Cardinal Industries, Inc., Milwaukee, WI, USA), using a two-wire probe. The distance between the noninsulated edges of the two wires of the probe was 14 mm. Voltage measured divided by the distance between the wire edges gives the induced electrical field figure. Stimulation was delivered using the Magstim Model 200 stimulator at 100% power level. The coils were placed on the glass surface and the electrical field was measured in numerous points within the saline solution.

RESULTS

The simulations revealed that, in general, the presence of accumulating surface charge induced by coil configurations having a radial current component changes the total field in a nontrivial way. The presence of an electrostatic field not only reduces the total field at any point, but also leads to significant reduction in the percentage of the total field in depth, relative to total

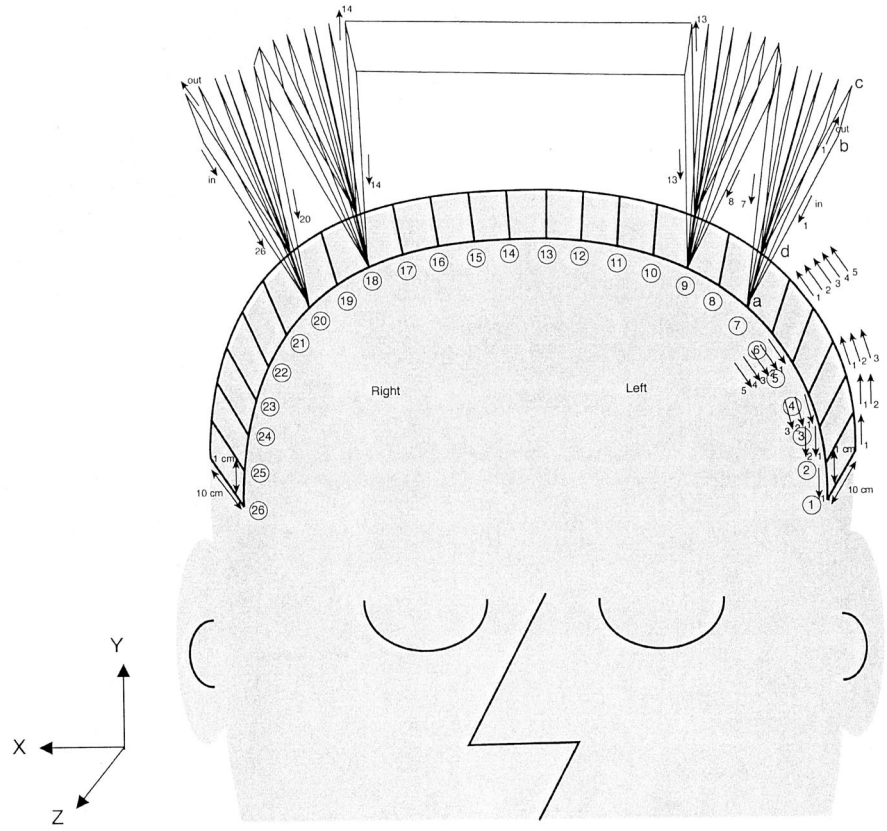

FIG. 2. The Hesed coil shape when applied over the human head. The same coil can be placed around the forehead to stimulate nerve fibers in the superoinferior direction. The only elements that produce an electrical field in the z-direction are the 26 strips attached to the head (numbered 1 to 26), where the current is in the +z direction, and the 26 return paths at the edges of the fans where the current is in the −z direction.

field at the surface. Moreover, both the total field and the percentage relative to the surface at any specific point depend on its distance from the nontangential coil elements. The basic concept of the new coil design is to generate summation of the electrical field in depth by inducing electrical fields at different locations around the surface of the head, all of which have a common direction. Such an approach increased the percentage of electrical field induced in depth, relative to the field in the surface regions. In addition, because a radial component had a dramatic effect on the percentage of the electrical field in depth, an effort was made to minimize the overall length of nontangential coil elements, and to locate them as distant as possible from the deep region to be activated. This region simulated the location of the nucleus accumbens. Calculations for several coil configurations were made and the optimal configuration (termed the *Hesed coil*) was compared with standard circular coils and with the double-cone coil. We compare simulation results of field distribution of the Hesed coil design (Fig. 2), of a double-cone coil, and of a circular coil oriented perpendicular (Fig. 3A) and parallel (Fig. 3B) to the head.

Fig. 2 shows the coil design when applied on the human head. The coil contains several strips (26 in the example of Fig. 2) attached to the head, all connected serially, and having wires that induce stimulation in the desired direction. This desired direction is the anteroposterior direction in the example shown in Fig. 2 (+z direction). For each strip there is a return path wire having current component at the opposite direction (−z direction), located 5 cm above the head. These return paths are located at the top edges of four fans, to remove the currents flowing through them away from the deep regions of the head. The specific design of the fans is meant to reduce the inductance of the coil. The fans are connected to the frame near strips 7, 9, 18, and 20 (see Fig. 2). These loci were chosen to remove the return paths as much as possible from the deep brain region to be activated most effectively. The only wires with cur-

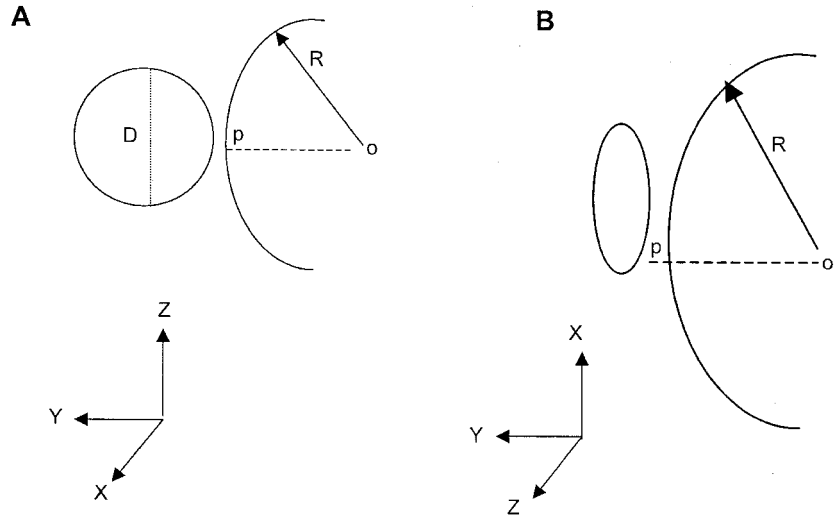

FIG. 3. (A) A circular coil with diameter D placed perpendicular to the head surface. The head is modeled as a sphere with a radius R = 7 cm. The coil has current component in the y-direction, which is perpendicular to the head, and a component in the z-direction, which is completely parallel to the head surface only at the attachment point p. **(B)** A circular coil with diameter D placed tangential to the head surface. The coil has current components in the x- and z-directions, which are completely parallel to the head surface only at the attachment point p.

rents that have radial components are those connecting the strips that are attached to the head with their return paths, along the sides of the fans. An optimized coil would have a flexible frame allowing all elements of the coil that are touching the head to be tangential to the head surface (see Fig. 2).

In the calculations of the field produced by the Hesed coil design, we assumed that the only coil elements carrying current components that are not tangential to the surface are the wires connecting the return paths with the strips that are attached to the head (along the fans). This is a plausible assumption in the realistic case, where the coil is attached to the skull. In the human head, the cerebral spinal fluid is approximately parallel to the skull everywhere and it can be assumed that the conductive properties of the cerebral spinal fluid are similar to those of the brain. The electrostatic field resulting from the contribution of the nontangential elements was calculated for each point and subtracted from the induced field of the coil.

To obtain maximal efficacy, given the limitations of the stimulator and the need for a specific range of the coil inductance (15 to 25 μH), the average lengths of the strips were taken as 8 cm. The simulations were made for strips length of 9 cm over one hemisphere and of 7 cm over the other hemisphere (to obtain a slight preference for one hemisphere stimulation and to have the opportunity to reach stimulation threshold in one hemisphere only). The wires connecting the head strips to their return paths (the nontangential elements) were taken as 5 cm long. The locations of the strips were determined to fit the human head, as in Fig. 2. Hence, the distances of strips 13 and 14 from the sphere center were taken as approximately 6 cm; strips 3 and 24 were located approximately 7 cm from the sphere center.

For the orientation shown in Fig. 2, the maximal total field in the anteroposterior direction (z direction) was produced at the cortex near the center of strips 1 and 26 at the sides. The field at the top of the head was reduced considerably because of the influence of the return paths and of the nontangential wires along the sides of the fans.

Fig. 4 shows the induced (Fig. 4A) and total (Fig. 4B) field in the z-direction (Ez, defined in Fig. 3) of a one-turn 5.5-cm-diameter circular coil placed perpendicular and parallel to a 7-cm-radius spherical volume conductor, as a function of distance from the coil edge. The fields were calculated along the line connecting the sphere center to the coil point closest to the surface (line o-p in Fig. 3). It is clear that the reduction in total field resulting from charge accumulation is much larger when the coil is oriented perpendicular to surface (Fig. 4). In addition, a comparison was made with the induced and total fields of one winding from the new Hesed coil, including strip 1 with its connection to the return path and its return path itself (and taking strips length of 5.5 cm). The simulations show that although the induced field of the strip is slightly larger than that of a circular coil with similar dimensions (see Fig. 4), the difference in the total field is much larger (see Fig. 4). This results from the fact that the field reduction due to electrostatic

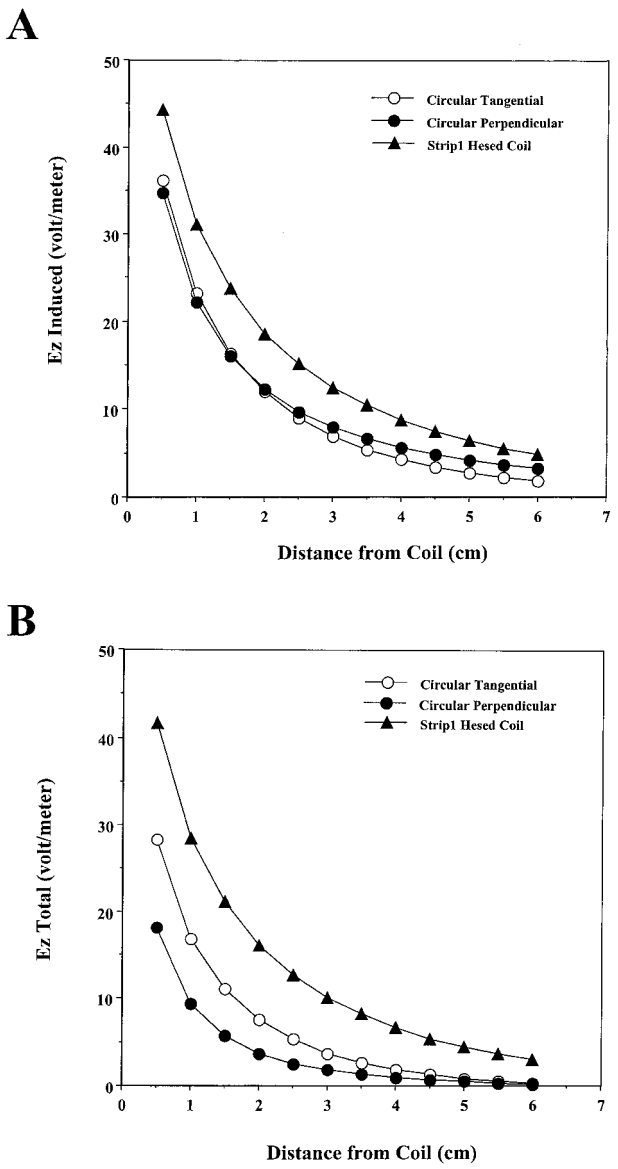

FIG. 4. (A, B) Induced **(A)** and total **(B)** electrical field in the z-direction plotted as a function of distance from a one-turn circular coil of 5.5-cm diameter placed tangential or perpendicular to the head surface. In addition the induced and total fields of the winding of the Hesed coil connected to strip 1 (see Fig. 2) is shown for the case of strip length of 5.5 cm.

charge accumulation in the case of the winding of strip 1 is very small, because the only elements carrying radial current components are the wires along paths a-b and c-d (see Fig. 2), which are a relatively small fraction of the winding length, and are distant from the points under consideration.

The induced and total field in z-direction (Ez) resulting from the entire Hesed coil compared with the double-cone coil is shown in Fig. 5. The field of the Hesed coil is computed along the line from strip 26 (where it is maximal) to the sphere center. The field of the double-cone coil is computed along the line from the junction at the coil center (where it is maximal) to the sphere center.

Although the double-cone coil produces a much larger induced field than the Hesed coil (see Fig. 5A), the rate of decay of the effective total field with distance is much smaller for the Hesed coil (see Fig. 5B). Hence, at depth of 6 cm, the total electrical field of the Hesed coil is already a little larger than that of the double-cone coil (see Fig. 5B).

Fig. 6 shows the z-component of the electrical field as a function of distance, relative to the field at a distance of 1 cm, for the Hesed coil, a double-cone coil with 14-cm diameter for each wing, and the 5.5-cm-diameter circular coil oriented tangential and perpendicular to the head surface. The field produced by the Hesed coil at a depth of 6 cm is approximately 35% of the field at a depth of 1 cm near the middle of strip 26 (where the field induced by the Hesed coil is highest throughout the brain). The field produced by the double-cone coil at a depth of 6 cm is only about 8% of the field 1 cm from the coil. The field produced by the 5.5-cm-diameter circular coil at this depth is less than 2% of the field 1 cm from the coil. For a larger circular coil, the percentage of field in depth is somewhat higher, but still smaller than that of the double-cone coil (data not shown).

Actual measurements of the electrical fields in a phantom brain using the first manufactured version of the Hesed coil and a double-cone coil basically confirmed our theoretical calculations. Both coils produced slightly lower fields at any point in the phantom brain compared with the theoretical calculations. However, this was more evident in the case of the Hesed coil, and the percentage of field in depth relative to the surface was slightly lower compared with our calculations. The results for the total field and the percentage in depth are presented in Fig. 7.

It is clear that the total field induced by the double-cone coil, using the maximal output of the stimulator (10,000 amps/100 μsec) produces a markedly greater electrical field up to 6 cm depth, compared with the Hesed coil (see Fig. 7A), but the percentage in depth is markedly greater when the Hesed coil is used (see Fig. 7B).

DISCUSSION

In general, both the theoretical calculations and the phantom measurements confirm that the percentage of the electrical field in deep relative to the superficial regions of a conductive sphere is significantly greater for

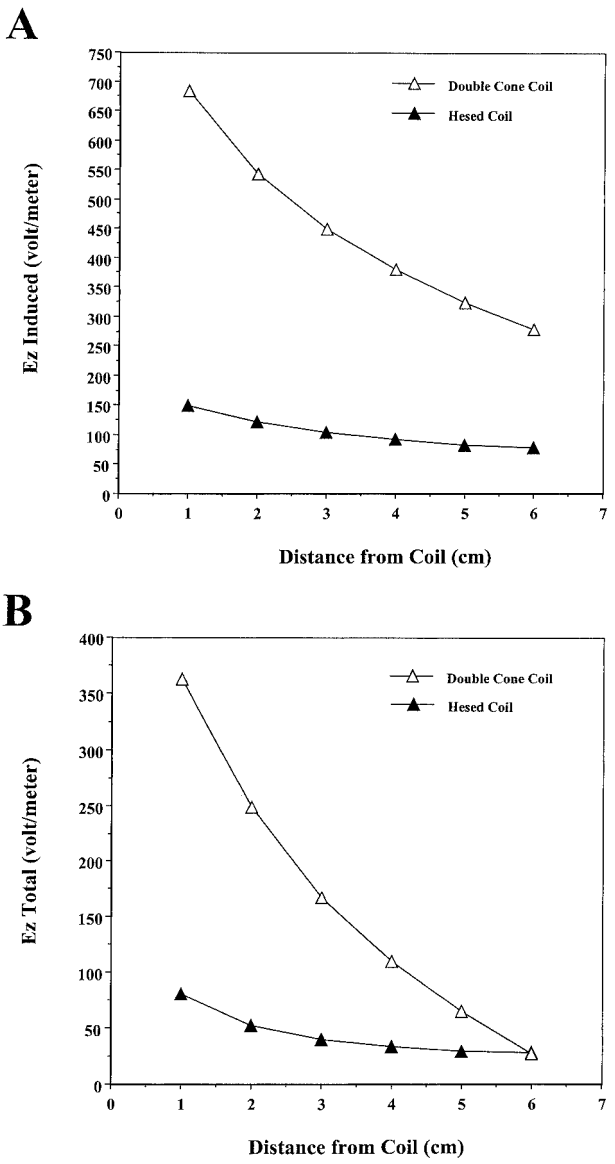

FIG. 5. (A, B) Induced **(A)** and total **(B)** electrical field in the z-direction plotted as a function of distance for the double-cone coil and the Hesed coil. The electrical fields were calculated for a six-turn double-cone coil with a diameter of 14 cm for each wing, an opening angle of 95 deg, and a central linear section of 3 cm, and for the Hesed coil with strip lengths of 9 cm over the right hemisphere and 7 cm over the left hemisphere. The field of the Hesed coil is computed along the line from strip 26 (where Ez is maximal) to the sphere center (see Fig. 2). The field of the double-cone coil is computed along the line from the central linear section (where Ez is maximal) to the sphere center.

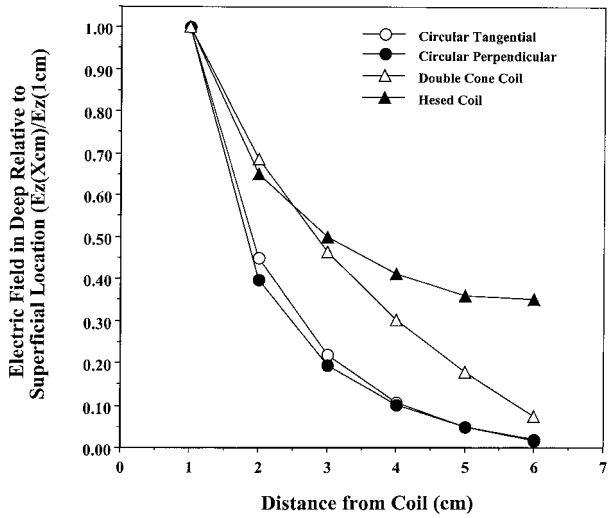

FIG. 6. Electrical field in the z-direction relative to the field 1 cm from the coil as a function of distance. Data are presented for the Hesed coil, the double-cone coil (both as described in Fig. 5), and the 5.5-cm-diameter circular coil oriented tangential and perpendicular to the head surface (as described in Figs. 3 and 4). The total electrical field in each point along the line from the point of maximal Ez to the sphere center was divided by the Ez value calculated at a 1-cm distance.

the new coil design compared with other coils including the double-cone coil. The reason for the small differences between the theoretical calculations and the phantom measurements may be related to the fact that the actual coil did not have a completely flexible frame, and therefore the strips were not strictly parallel to the phantom brain model. In addition the phantom brain shape was slightly different from the spherical volume conductor model used in the simulations.

To reach the stimulation threshold of neurons, a total field of 20 to 60 V/m is needed, and therefore, 30 to 50% of the maximal output of the Magstim stimulator is required when using a double-cone coil to stimulate the leg motor area, which is approximately 3 to 4 cm in depth (Maccabee et al., 1990; Terao et al., 1994, 2000). Such stimulation is painful because a much higher field is induced in higher cortical areas and facial muscles. To reach a stimulation threshold at a depth of 5 to 7 cm, a much higher intensity would be needed that would increase pain and the risk for other side effects. On the other hand, the total field induced in cortical regions by the Hesed coil is four times lower than that of the double-cone coil (even at maximal power output). Therefore, it is likely that excitation threshold can be reached at 5 to 7 cm using the Hesed coil without inducing pain and other side effects. The percentage of the electrical field in depth calculated for standard circular or figure-of-eight coils is even lower than that of the double-cone coil. Therefore, such coils would not only cause greater side effects, but could not reach stimulation threshold in depth, even when the maximal power output of the stimulator is used.

The fact that the double-cone coil has relatively more

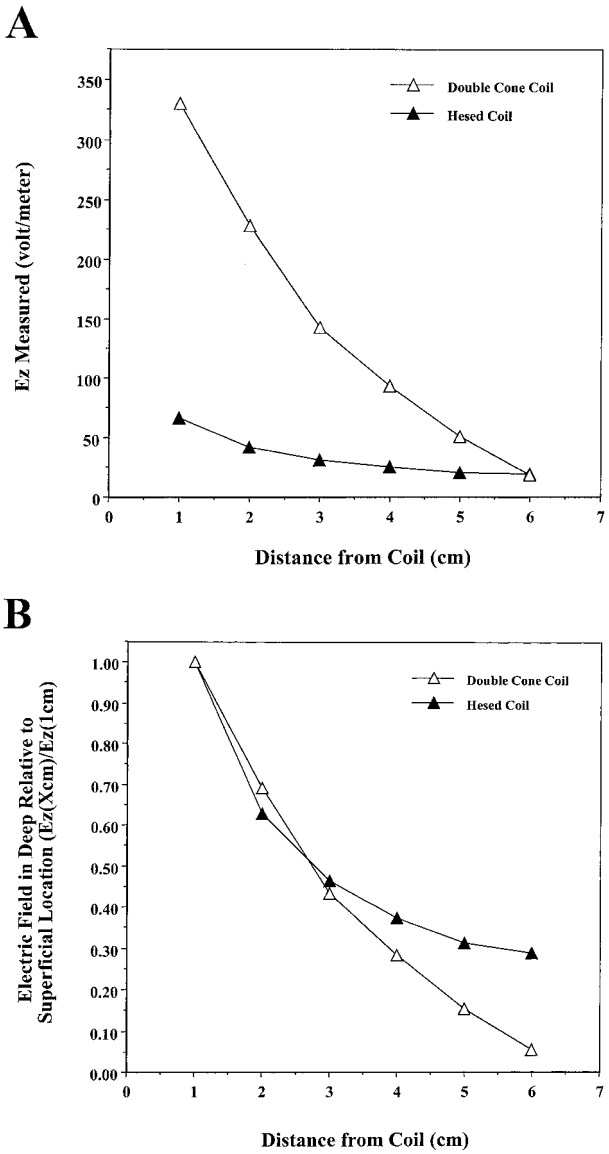

FIG. 7. Measurements of the electrical field induced by the Hesed coil and the double-cone coil in a phantom brain. **(A, B)** The electrical field induced in the z-direction **(A)** and the electrical field in the z-direction *relative* to the field 1 cm from the coil **(B)** is plotted as a function of distance from the coil. For both coils, the data show the measurements along the line from the point where maximal Ez value is obtained (as described earlier) to the sphere center.

nontangential current components than the Hesed coil leads to more significant reduction both in absolute field magnitude at any point and in the percentage of the deep region field relative to field at the surface. In general, the reduction in total field resulting from the electrostatic field diminishes as the stimulated point is farther from the coil elements, which carry nontangential current components. It also depends on the relative fraction of the field at the stimulated point that is produced by coil elements carrying such currents. Hence, the field at the sides (near strips 1 and 26) was the highest field induced by the Hesed coil anywhere inside the head. The field in other cortical regions is considerably smaller.

Among available coils, the decrease in electrical field with distance inside a homogeneous volume conductor is faster for a figure-of-eight coil than for a circular coil oriented tangential to the surface (Cohen et al., 1989; Maccabee et al., 1989). The family of coils termed *slinky coils*, which are actually intermediate configurations between a figure-of-eight coil tangential to and a circular coil perpendicular to tissue surface (Ren et al., 1995; Zimmermann et al., 1996) give no advantage in terms of depth stimulation. The double-cone coil may be viewed as a particularly large type of the slinky coil. In general, for every coil configuration, increasing the coil dimensions would increase the penetration of the electrical field in depth, but the stimulated tissue area will also increase.

The electrical field produced by the Hesed coil in the brain may be increased significantly by screening the electrical field induced by the return paths (which are 5 cm above the head; see Fig. 2). Such screening may be obtained by inserting insulated metal flasks near the return paths. This would also increase the percentage of electrical field in depth because the negative effect of the return paths is *relatively* greater in depth. The decrease of field with distance from the Hesed coil is fastest close to the strips and slower in depth. Hence, the coil frame can be placed farther from the skull (1.5 to 2 cm) to obtain an even higher percentage of fields in depth relative to cortical fields.

The Hesed coil may be used to stimulate a variety of deep brain regions. The exact coil configuration and placement may depend on the application. For instance, activation of deep neuronal bundles along the anteroposterior axis would be achieved by placing the coil over a coronal slice, as shown in Fig. 2. Activation of deep neuronal bundles along the superoinferior axis (e.g., cingulate–accumbens fibers) would be achieved by placing the coil over an axial slice, and an optimized coil shape for such purpose may surround an entire axial slice of the head. The return paths should be placed as distant as possible from the brain region designated for activation.

REFERENCES

Basser PJ, Roth BJ. Stimulation of a myelinated nerve axon by electromagnetic induction. *Med Biol Eng Comput* 1991;29:261–8.
Branston NM, Tofts PS. Analysis of the distribution of currents

induced by a changing magnetic field in a volume conductor. *Phys Med Biol* 1991;36:161–8.
Branston NM, Tofts PS. Magnetic stimulation of a volume conductor produces a negligible component of induced current perpendicular to the surface. *J Physiol (Lond)* 1990;423:67.
Breiter HC, Gollub RL, Weisskoff RM, et al. Acute effects of cocaine on human brain activity and emotion. *Neuron* 1997;19:591–611.
Breiter HC, Rosen BR. Functional magnetic resonance imaging of brain reward circuitry in the human. *Ann N Y Acad Sci* 1999;877: 523–47.
Cohen D, Cuffin BN. Developing a more focal magnetic stimulator. Part I: some basic principles. *J Clin Neurophysiol* 1991;8:102–11.
Cohen LG, Roth BJ, Nilsson J, et al. Effects of coil design on delivery of focal magnetic stimulation. Technical considerations. *Electroencephalogr Clin Neurophysiol* 1990;75:350–7.
Eaton H. Electric field induced in a spherical volume conductor from arbitrary coils: application to magnetic stimulation and MEG. *Med Biol Eng Comput* 1992;30:433–40.
Ikemoto S, Panksepp J. The role of nucleus accumbens dopamine in motivated behavior: a unifying interpretation with special reference to reward-seeking. *Brain Res Rev* 1999;31:6–41.
Jacques S. Brain stimulation reward: "pleasure centers" after twenty-five years. *Neurosurgery* 1999;5:277–83.
Jentsch JD, Taylor JR. Impulsivity resulting from frontostriatal dysfunction in drug abuse: implications for the control of behavior by reward-related behaviors. *Psychopharmacology* 1999;146: 373–90.
Kalivas PW, Nakamura M. Neural systems for behavioral activation and reward. *Curr Opin Neurobiol* 1999;9:223–7.
Kirkcaldie MT, Pridmore SA, Pascual–Leone A. Transcranial magnetic stimulation as therapy for depression and other disorders. *Aust N Z J Psychiatry* 1997;31:264–72.
Lyons D, Friedman DP, Nader MA, Porrino LJ. Cocaine alters cerebral metabolism within the ventral striatum and limbic cortex of monkeys. *J Neurosci* 1996;16:1230–8.
Maccabee PJ, Eberle L, Amassian VE, Cracco RQ, Rudell A, Jayachandra M. Spatial distribution of the electric field induced in volume by round and figure '8' magnetic coils: relevance to activation of sensory nerve fibers. *Electroencephalogr Clin Neurophysiol* 1990;76:131–41.
Milner PM. Brain-stimulation reward: a review. *Can J Psychol* 1991; 45:1–36.
Ren C, Tarjan PP, Popovic DB. A novel electric design for electromagnetic stimulation: The slinky coil. *IEEE Trans Biomed Eng* 1995;42:918–25.
Roth BJ, Basser PJ. A model of the stimulation of a nerve fiber by electromagnetic radiation. *IEEE Trans Biomed Eng* 1990;37:588–97.
Roth BJ, Cohen LG, Hallet M, Friauf W, Basser PJ. A theoretical calculation of the electric field induced by magnetic stimulation of a peripheral nerve. *Muscle Nerve* 1990;13:734–41.
Ruhonen J, Ilmoniemi RJ. Focusing and targeting of magnetic brain stimulation using multiple coils. *Med Biol Eng Comput* 1998;38: 297–301.
Schultz W, Dayan P, Montague PR. A neural substrate of prediction and reward. *Science* 1997;275:1593–9.
Self DW, Nestler EJ. Molecular mechanisms of drug reinforcement and addiction. *Annu Rev Neurosci* 1995;18:463–95.
Stokic DS, McKay WB, Scott L, Sherwood AM, Dimitrijevic MR. Intracortical inhibition of lower limb motor-evoked potentials after paired transcranial magnetic stimulation. *Exp Brain Res* 1997;117:437–43.
Terao Y, Ugawa Y, Hanajima R, et al. Predominant activation of I1-waves from the leg motor area by transcranial magnetic stimulation. *Brain Res* 2000;859:137–46.
Terao Y, Ugawa Y, Sakai K, Uesaka Y, Kanazawa I. Transcranial magnetic stimulation of the leg area of motor cortex in humans. *Acta Neurol Scand* 1994;89:378–83.
Tofts PS. The distribution of induced currents in magnetic stimulation of the brain. *Phys Med Biol* 1990;35:1119–28.
Tofts PS, Branston NM. The measurement of electric field, and the influence of surface charge, in magnetic stimulation. *Electroencephalogr Clin Neurophysiol* 1991;81:238–9.
Volkow ND, Fowler JS. Addiction, a disease of compulsion and drive: involvement of the orbitofrontal cortex. *Cereb Cortex* 2000;10: 318–25.
Wassermann EM, Lisanby SH. Therapeutic application of repetitive transcranial magnetic stimulation: a review. *Clin Neurophysiol* 2001;112:1367–77.
Zimmermann KP, Simpson RK. "Slinky" coils for neuromagnetic stimulation. *Electroencephalogr Clin Neurophysiol* 1996;101: 145–52.